

Inverse Method for Estimating the Spatial Variability of Soil Particle Size Distribution from Observed Soil Moisture

Feifei Pan¹; Christa D. Peters-Lidard²; and Anthony W. King³

Abstract: Soil particle size distribution (PSD) (i.e., clay, silt, sand, and rock contents) information is one of critical factors for understanding water cycle since it affects almost all of water cycle processes, e.g., drainage, runoff, soil moisture, evaporation, and evapotranspiration. With information about soil PSD, we can estimate almost all soil hydraulic properties (e.g., saturated soil moisture, field capacity, wilting point, residual soil moisture, saturated hydraulic conductivity, pore-size distribution index, and bubbling capillary pressure) based on published empirical relationships. Therefore, a regional or global soil PSD database is essential for studying water cycle regionally or globally. At the present stage, three soil geographic databases are commonly used, i.e., the Soil Survey Geographic database, the State Soil Geographic database, and the National Soil Geographic database. Those soil data are map unit based and associated with great uncertainty. Ground soil surveys are a way to reduce this uncertainty. However, ground surveys are time consuming and labor intensive. In this study, an inverse method for estimating mean and standard deviation of soil PSD from observed soil moisture is proposed and applied to Throughfall Displacement Experiment sites in Walker Branch Watershed in eastern Tennessee. This method is based on the relationship between spatial mean and standard deviation of soil moisture. The results indicate that the suggested method is feasible and has potential for retrieving soil PSD information globally from remotely sensed soil moisture data.

DOI: 10.1061/(ASCE)HE.1943-5584.0000274

CE Database subject headings: Particle size distribution; Soil water; Moisture; Inverse method; Spatial analysis.

Author keywords: Soil particle size distribution (PSD); Soil moisture; Inverse method.

Introduction

Soil particle size distribution (PSD) provides information about clay, silt, sand, and rock contents. According to the USDA particle size limit classification scheme (USDA-SCS 1982), the sizes of clay, silt, sand, and rock are 0.0002–0.002, 0.002–0.05, 0.05–2.0, and >2.0 mm, respectively. To determine soil texture by the proportions of sand, silt, and clay, particles larger than sand (i.e., >2.0 mm) are first removed. Since the sum of percentages of clay, silt, and sand contents is equal to 100%, the percentage of silt content can be estimated from clay and sand contents. Therefore, hereafter, soil PSD is referred to clay, sand, and rock contents.

Soil PSD is a critical factor for understanding the cycling of water through terrestrial ecosystems because we can estimate other soil hydraulic properties based on soil PSD information (e.g., Rawls et al. 1982, 1989 and Saxton et al. 1986). Soil properties affect almost all water cycle processes, including drainage, runoff, soil moisture content, evaporation, and transpiration. Understanding regional or global spatially extensive water cycling

requires a geographically distributed soil PSD database. At present, three large-scale soil databases are commonly used in the United States: the Soil Survey Geographic (SSURGO) database, the State Soil Geographic (STATSGO) database, and the National Soil Geographic (NATSGO) database. These soil data are “map unit based.” Each map unit can have multiple components, and the percentage of each component is given in an attribute table. Since the geographic location of each soil component is not specified, we can only determine the soil PSD of each map unit using the weighted average of all soil components.

For example, a map unit has n soil components. We use S_i , C_i , and R_i to represent the percentages of sand, clay, and rock for component i and A_i to represent the distributional area coverage of component i . Using the weighted average method, we can estimate the mean PSD of the map unit as follows:

$$\bar{S} = \frac{\sum_{i=1}^n A_i S_i}{\sum_{i=1}^n A_i}; \quad \bar{C} = \frac{\sum_{i=1}^n A_i C_i}{\sum_{i=1}^n A_i}; \quad \bar{R} = \frac{\sum_{i=1}^n A_i R_i}{\sum_{i=1}^n A_i} \quad (1)$$

However, this method is questionable when the study domain is not the same as the map unit. Moreover, we cannot estimate the variance or standard deviation of the soil PSD for the map unit because those soil databases do not provide any information on spatial variance of soil properties of each soil component and spatial correlation among soil components, while the soil spatial variability affects the spatial pattern of hydrological processes significantly (e.g., Sharma and Luxmoore 1979; Milly and Eagleson 1987).

A soil survey is one way to determine the mean and variance of soil properties (e.g., Edmonds et al. 1982, 1985; Edmonds and

¹Dept. of Geography, Univ. of North Texas, Denton, TX 76203 (corresponding author). E-mail: feifei.pan@unt.edu

²Hydrological Sciences Branch, NASA Goddard Space Flight Center, Greenbelt, MD 20771.

³Environmental Science Division, MS 6335, Oak Ridge National Laboratory, Oak Ridge, TN 37831-6335.

Note. This manuscript was submitted on May 6, 2009; approved on April 28, 2010; published online on May 14, 2010. Discussion period open until April 1, 2011; separate discussions must be submitted for individual papers. This paper is part of the *Journal of Hydrologic Engineering*, Vol. 15, No. 11, November 1, 2010. ©ASCE, ISSN 1084-0699/2010/11-931-938/\$25.00.

Lentner 1986; Cambardella et al. 1994; Young et al. 1997, 1998). Although a soil survey is relatively simple, it is time consuming and labor intensive. As a consequence, the availability of comprehensive and consistent surveys over large spatial extents is quite limited. Nevertheless, a soil survey provides a spatially distributed sample of point measurements. These point measurements provide the basic information on soil properties needed by hydrological models but to apply this information to a large-scale hydrologic model, we need to estimate the “effective” soil hydraulic properties from the point measurements (e.g., Milly and Eagleson 1987; Yeh 1989; Kim et al. 1997; Zhu and Mohanty 2003). The effective soil properties are the integrated soil properties of the computational elements with larger areas than the sample points of soil surveys, e.g., basins, watersheds, catchments, or grid cells. However, capturing the high spatial heterogeneity of soil characteristics in the estimated effective soil parameters requires a highly dense soil sampling network. This increases the difficulty and expense of extracting effective soil properties directly from soil survey point data.

Remote sensing of soil PSD is a potential solution to this problem. Some studies have shown the ability of satellite spectral imagery to quantify clay and sand contents over large areas using spectral analysis (e.g., Palacios-Orueta and Ustin 1998 and others). However, the perennial issues of how clouds and atmosphere affect satellite imagery limit this approach, adding a different, nonsampling source of uncertainty in estimating soil texture.

Another alternative and the one we investigate here is to retrieve the soil PSD information through “inversion” of microwave remotely sensed soil moisture. If we consider the observed soil moisture as an output signal of a system due to an input signal such as precipitation, radiation, and other forcing, it is an inverse problem (Santamarina and Fratta 1998) to determine the system characteristics (e.g., soil PSD) from the output (i.e., soil moisture) only or a combination of input and output. Feddes (1995) used an inverse modeling approach to determine large-scale effective soil hydraulic properties by fitting simulated soil moisture to remotely sensed soil moisture. However, Feddes’ dependency on a soil-water-vegetation-atmosphere (SWVA) model and the large data requirement for running the model make this particular inverse modeling approach difficult to implement.

Chang and Islam (2000) and Chang et al. (2003) applied the artificial neural network models to retrieve soil texture information from microwave remotely sensed brightness temperature. However, a wide variation of soil PSD associated with each soil texture classification indicates that using only soil texture information could create a large uncertainty in hydrological modeling.

In this paper, we instead propose a simple inverse method to estimate mean and variance of soil PSD from observed soil moisture fields without running an SWVA model. The fundamental goal is to apply this method to remotely sensed soil moisture. However, since the remote sensing techniques on soil moisture are still at the developing stage, the characteristics of short sampling periods and few measurements during wet periods make it difficult to use remotely sensed soil moisture for demonstrating our methodology in this paper. In this study, we use existing soil moisture observations for a mesic deciduous forest system in the eastern United States to demonstrate our methodology. The soil moisture measurements were collected on a (80 m × 160 m) plot with 200 regular grid cells (8-m spacing), which can be thought as remotely sensed soil moisture images with an 8-m resolution. The detailed information is given in the study area and data section. With the increasing availability of remotely sensed soil moisture data, an easily implemented methodology for extracting

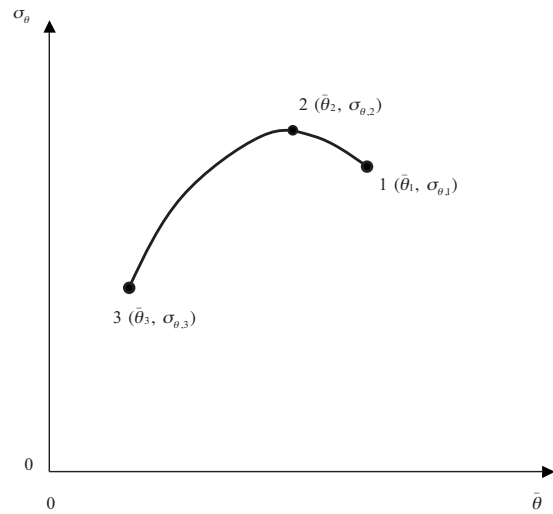


Fig. 1. Schematic plot of the relationship between spatial mean and standard deviation of soil moisture fields

soil PSD information promises an attractive alternative to costly soil surveys and reduces uncertainty in the map unit based geographical soil databases.

Methods

Our proposed method is based on the relation between mean and standard deviation of soil moisture. Through analyzing observed soil moisture and studying the effects of the spatial variability of soil texture on spatial variation of soil moisture, Pan and Peters-Lidard (2008) found that the relation between the spatial mean and standard deviation of soil moisture depends on the mean soil moisture state. As the mean soil moisture varies between saturated soil moisture and field capacity, the standard deviation increases with decreasing mean soil moisture; but when mean soil moisture is between the field capacity state and residual soil moisture, standard deviation decreases with decreasing mean soil moisture. The transition state is the field capacity at which evaporation over bare soil or evapotranspiration over vegetated surface switches from the potential rate to the actual rate limited by soil-water content.

Since most observed soil moisture is between the states of saturation and wilting point, we can construct the relationship between the mean and standard deviation with three points: saturation point (1: $\bar{\theta}_1, \sigma_1$), transition state (2: $\bar{\theta}_2, \sigma_2$), and wilting point (3: $\bar{\theta}_3, \sigma_3$) (Fig. 1). These points are defined by the mean and standard deviation of soil moisture at (1) saturation, (2) field capacity, and (3) wilting point, respectively.

According to Pan and Peters-Lidard (2008), the variance or standard deviation at Point 2 is a maximum. Therefore, we can use a third-order polynomial to fit the scatter plot of mean and standard deviation and force the best-fit (least-squares) curve through those three points and with a local maximum at Point 2. This expression is given by

$$\sigma_{\theta} = f_0 + f_1 \bar{\theta} + f_2 \bar{\theta}^2 + f_3 \bar{\theta}^3 \quad (2)$$

The parameters $f_0, f_1, f_2,$ and f_3 satisfy the following equations:

$$\sigma_i = f_0 + f_1 \bar{\theta}_i + f_2 \bar{\theta}_i^2 + f_3 \bar{\theta}_i^3 \quad (i = 1, 2, \text{ and } 3) \quad (3)$$

$$\left. \frac{\partial \sigma}{\partial \bar{\theta}} \right|_2 = f_1 + 2f_2\bar{\theta}_2 + 3f_3\bar{\theta}_2^2 = 0 \quad (4)$$

$$\theta = (1 - R/100) \left(\frac{|\Psi|}{A} \right)^{1/B} \quad (13)$$

We solve Eqs. (3) and (4) and have the following:

$$f_0 = \sigma_1 + \frac{(2\bar{\theta}_1\bar{\theta}_2 - \bar{\theta}_1\bar{\theta}_1)(SI)}{(\bar{\theta}_1 - \bar{\theta}_2)} - \bar{\theta}_1\bar{\theta}_2\bar{\theta}_2f_3 \quad (5)$$

$$f_1 = \frac{-2\bar{\theta}_2(SI)}{(\bar{\theta}_1 - \bar{\theta}_2)} + (\bar{\theta}_2\bar{\theta}_2 + 2\bar{\theta}_2\bar{\theta}_1)f_3 \quad (6)$$

$$f_2 = \frac{SI}{(\bar{\theta}_1 - \bar{\theta}_2)} - (\bar{\theta}_1 + 2\bar{\theta}_2)f_3 \quad (7)$$

$$f_3 = \frac{SW}{(\bar{\theta}_2 - \bar{\theta}_3)^2} - \frac{(\bar{\theta}_3 + \bar{\theta}_1 - 2\bar{\theta}_2)(SI)}{(\bar{\theta}_2 - \bar{\theta}_3)^2(\bar{\theta}_1 - \bar{\theta}_2)} \quad (8)$$

where $SW = (\sigma_1 - \sigma_3)/(\bar{\theta}_1 - \bar{\theta}_3)$ and $SI = (\sigma_1 - \sigma_2)/(\bar{\theta}_1 - \bar{\theta}_2)$.

Prior to inverting Eq. (2) with parameters given by Eqs. (5)–(8) to estimate mean and standard deviation of soil PSD, we first derive the analytical relationships among the mean and standard deviation of soil PSD and soil moisture fields at the three states. Soil moisture (θ) content at a certain hydraulic state can be expressed as a function of sand (S), clay (C), and rock (R)

$$\theta = f(S, C, R) \quad (9)$$

where C , S , and R stand for the percentages (%) of clay, sand, and rock. We use $\rho_{S,C}$ to denote the correlation coefficient between sand and clay and assume that there is no correlation between rock content and sand, or rock content and clay. Applying Taylor's expansion to Eq. (9) (Benjamin and Cornell 1970), we can estimate a soil moisture mean ($\bar{\theta}$) and standard deviation (σ_θ) as follows:

$$\bar{\theta} = f(\bar{S}, \bar{C}, \bar{R}) + \left[\frac{1}{2}\sigma_S^2 \frac{\partial^2 \theta}{\partial S^2} + \frac{1}{2}\sigma_C^2 \frac{\partial^2 \theta}{\partial C^2} + \frac{1}{2}\sigma_R^2 \frac{\partial^2 \theta}{\partial R^2} + \rho_{S,C}\sigma_S\sigma_C \frac{\partial^2 \theta}{\partial S \partial C} \right] \Bigg|_{S=\bar{S}, C=\bar{C}, R=\bar{R}} \quad (10)$$

$$\sigma_\theta^2 = \left[\sigma_S^2 \left(\frac{\partial \theta}{\partial S} \right)^2 + \sigma_C^2 \left(\frac{\partial \theta}{\partial C} \right)^2 + \sigma_R^2 \left(\frac{\partial \theta}{\partial R} \right)^2 + 2\rho_{S,C}\sigma_S\sigma_C \frac{\partial \theta}{\partial S} \frac{\partial \theta}{\partial C} \right] \Bigg|_{S=\bar{S}, C=\bar{C}, R=\bar{R}} \quad (11)$$

Relations between soil-water potential and soil-water content have been widely studied and well documented in the literature (e.g., Rawls et al. 1982; Saxton et al. 1986). In this study, we use the soil-water potential relationship with soil-water content of Saxton et al. (1986) to determine soil moisture at saturation, field capacity, and wilting point. Soil moisture at saturation is given as

$$\theta_s = (1 - R/100)[c_1 + c_2S + c_3 \ln(C)/\ln(10)] \quad (12)$$

where $c_1 = 0.332$, $c_2 = -7.251 \times 10^{-4}$, and $c_3 = 0.1276$.

As the pressure head ψ is between -10 and $-1,500$ kPa, the soil moisture is given as (Saxton et al. 1986)

where $A = 100 \exp(c_4 + c_5C + c_6S^2 + c_7S^2C)$, $B = c_8 + c_9C^2 + c_{10}S^2C$, $c_4 = -4.396$, $c_5 = -0.0715$, $c_6 = -4.880 \times 10^{-4}$, $c_7 = -4.285 \times 10^{-5}$, $c_8 = -3.140$, $c_9 = -2.22 \times 10^{-3}$, and $c_{10} = -3.484 \times 10^{-5}$.

Based on Eqs. (10) and (11) and soil moisture retention equations (12) and (13), we can derive mean and standard deviation of soil moisture at saturation, field capacity, and wilting point as functions of mean and standard deviation of soil PSD. The detailed derivation is given in the Appendix.

Applying the expressions of mean and standard deviation of soil moisture at saturation, transition, and wilting points (see Appendix) to Eqs. (5)–(8) and substituting them into Eq. (2), we obtain an expression of standard deviation of soil moisture fields as a function of mean soil moisture, and mean and standard deviation of sand, clay and rock contents, and correlation coefficient between sand and clay

$$\sigma_\theta = F(\bar{\theta}, \bar{S}, \bar{C}, \bar{R}, \sigma_S, \sigma_C, \sigma_R, \rho_{S,C}) \quad (14)$$

To invert this equation and estimate mean and standard deviation of sand, clay, and rock contents from the observed soil moisture (i.e., $\bar{\theta}_i$ and σ_{θ_i}), we need to fit the scatter plot of mean and standard deviation of observed soil moisture fields with Eq. (14) by minimizing the root-mean-squared error (RMSE) given as follows:

$$\text{RMSE} = \sqrt{\frac{1}{n} \sum_{i=1}^n [\sigma_{\theta,i} - F(\bar{\theta}_i, \bar{S}, \bar{C}, \bar{R}, \sigma_S, \sigma_C, \sigma_R, \rho_{S,C})]^2} \quad (15)$$

where n = number of observed soil moisture mean and standard deviation, i.e., using n pairs of observed data ($\bar{\theta}_i, \sigma_{\theta,i}, i = 1, \dots, n$) to determine seven unknowns (i.e., \bar{S} , \bar{C} , \bar{R} , σ_S , σ_C , σ_R , and $\rho_{S,C}$).

Two methods can be used to achieve the best fit, i.e., Gauss-Newton method (Fletcher 1987) or simple "global search" methods. To use the Gauss-Newton method to minimize the nonlinear RMSE function given in Eq. (15), we need first to construct a Jacobian matrix. However, seven unknown parameters and high nonlinearity of Eq. (15) make it difficult to obtain an analytical expression of the Jacobian matrix. Compared to the Gauss-Newton method, the global search methods are simple. On the other hand, the best-fit solution of Eq. (15) using the Gauss-Newton method could be trapped in secondary minima. This problem can be avoided when using a global search method (Mosegaard and Tarantola 1995).

There are several methods for a global search. The simplest method is to exhaustively search the parameter space of unknown parameters. Although this method is simple and efficient for problems with few parameters, the computation becomes unfeasible for problems with many parameters (Mosegaard and Tarantola 1995). To inverse a nonlinear equation with high dimensionality (i.e., many parameters), we can use a Monte Carlo search, i.e., a random walk in the parameter space. Although the concept of the Monte Carlo method is simple and not new, it has been widely used to solve inverse problems, especially in seismology (e.g., Keilis-Borok and Yanovskaya 1967; Press 1968; Rothman 1985, 1986; Cary and Chapman 1988; Landa et al. 1989; Mosegaard and Vestergaard 1991; Koren et al. 1991). Because the main objective of this paper is to demonstrate the feasibility of the suggested method, we use the simple and feasible Monte Carlo search method here.

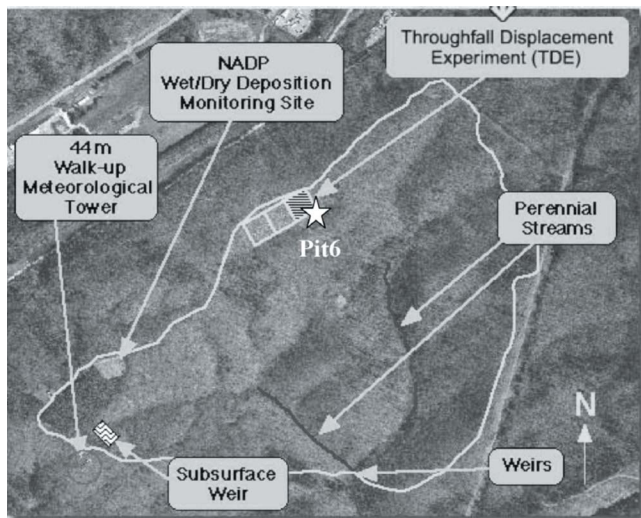


Fig. 2. TDE domain and Pit 6

Study Area and Data

Since 1993 a field experiment has been conducted in an upland oak forest on the Walker Branch Watershed (WBW) in eastern Tennessee to identify important ecosystem responses that might result from future precipitation changes (Hanson et al. 1998, 2003). On an 8 m × 8 m grid, volumetric soil moisture at 0–35 cm is being monitored with time domain reflectometers (TDR) at 310 sampling locations inside the throughfall displacement experiment (TDE) domain shown in Fig. 2. To eliminate the treatment effects (the shaded area shown in Fig. 2) we only use soil moisture measurements collected in the area without treatment. Therefore, we have 200 sampling points to represent an area of 80 m × 160 m. The TDR soil moisture measurements were made on 107 days (approximately once per month) from 1993 to 2000 at each sampling point. However, among these 107 days, only 95 days have more than 50% (i.e., 100) sampling points that have good measurements. To obtain a representative mean and standard deviation of soil moisture, we only used the data collected during those 95 days. The data are available at WBW TDE website (<http://tde.ornl.gov/>).

There are two soil PSD data sets, which can be downloaded from the WBW TDE website, available for validation of our method. One is rock content (0–30-cm) measurement at each soil moisture sampling site (Hanson et al. 1998). Mean and standard deviation of the measured rock contents are listed in Table 1. The other data set is a soil survey conducted by Peters et al. (1970) at 13 pits inside WBW. Among those 13 pits, only Pit 6 is close to the TDE site, which is marked in Fig. 2. The measured soil PSD at Pit 6 is shown in Table 1.

Table 1. Measured and Inversely Estimated Soil PSD

	\bar{S} (%)	\bar{C} (%)	\bar{R} (%)	σ_S (%)	σ_C (%)	σ_R (%)	$\rho_{S,C}$
Pit 6	19.2	5.9	26.6				
Measured			14.3			3.3	
Estimated	20.5	7.1	22.3	13.0	2.4	7.5	0.7

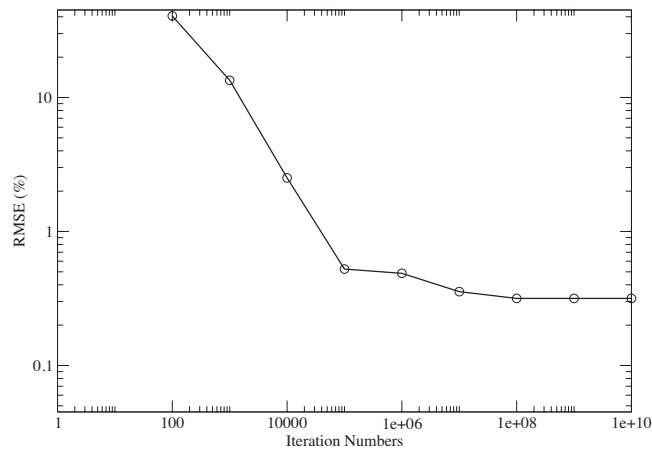


Fig. 3. Plot of the iteration number and the RMSE

Results and Discussions

As discussed in the Methods section, in this study we use the Monte Carlo method to search the optimal values of seven unknowns (i.e., \bar{S} , \bar{C} , \bar{R} , σ_S , σ_C , σ_R , and $\rho_{S,C}$) for a minimum RMSE between observed and predicted σ_θ . The searching domain is given as $0 \leq \bar{S} \leq 100$, $0 \leq \sigma_S \leq 100$, $0 \leq \bar{C} \leq 100$, $0 \leq \sigma_C \leq 100$, $0 \leq \bar{R} \leq 100$, $0 \leq \sigma_R \leq 100$, and $-1 \leq \rho_{S,C} \leq 1$. Fig. 3 shows that as the number of iteration increases, the RMSE of the estimated σ_θ decreases. As the number of iteration reaches 10^8 , the RMSE reaches its minimum value (0.32%) and does not decrease with increasing iteration number. The resulted PSD associated with the minimum RMSE is listed in Table 1. Fig. 4 shows the scatter plot of the mean and standard deviation of observed soil moisture at WBW TDE sites. The best-fit curve is also shown in Fig. 4.

Since the measured soil PSD at Pit 6 is a point measurement and the estimated soil PSD is associated with an area, we only can compare the estimated mean PSD with the observed PSD at Pit 6. According to Table 1, we can find that Pit 6's PSD is generally in the range of the estimated mean soil PSD ± 1 standard deviation. Another comparison is between the estimated and observed mean and standard deviation of rock content (\bar{R} , σ_R), as shown in

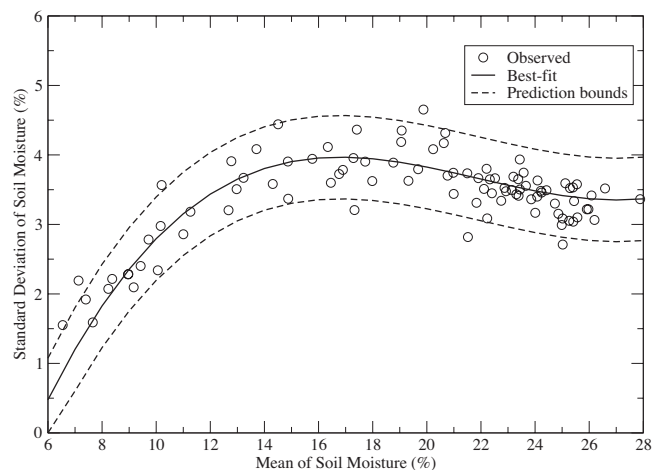


Fig. 4. Scatter plot of mean and standard deviation of observed soil moisture, the best-fit curve (solid), and 95% confidence interval (dashed)

Table 2. Average Values and 95% Confidence Limits of the Inversely Estimated Soil PSD Based on 1,000 Random Generated Soil Moisture Data Sets

	\bar{S} (%)	\bar{C} (%)	\bar{R} (%)	σ_S (%)	σ_C (%)	σ_R (%)	ρ_{SC}
Average	20.4	7.0	22.4	13.3	2.5	7.6	0.7
Lower limit	19.9	6.3	22.1	12.6	2.3	7.4	0.6
Upper limit	20.9	7.7	22.8	14.0	2.6	7.9	0.8

Table 1. Although the inversely retrieved mean and standard deviation of the rock content are little overestimated, the measured mean rock content is in the range of the estimated $\bar{R} \pm 1$ standard deviation.

To assess parameter identifiability and reliability, we also conducted an error analysis to determine the 95% confidence limits of the estimated parameters. We first determined the 95% confidence interval of the best-fit curve (i.e., predicted standard deviation of soil moisture) and plotted the upper bound and lower bound in Fig. 4. Using this 95% confidence interval, we generated 1,000 data sets. Each data set has 95 pairs of the mean and standard deviation of soil moisture ($\bar{\theta}_i, \sigma_{\theta,i}, i=1, \dots, 95$), where the mean soil moisture is the same as the observed mean soil moisture, and the associated standard deviation of soil moisture was randomly generated within the 95% confidence interval of the predicted standard deviation of soil moisture, as shown in Fig. 4. The Monte Carlo search method was applied to each data set to retrieve seven soil PSD parameters. The average values and 95% confidence limits of estimated seven soil PSD parameters from those 1,000 data sets are listed in Table 2. They are close to the estimated “true” soil PSD values listed in Table 1. The results of this error analysis indicate that the proposed method is capable of identifying soil PSD from the mean and standard deviation of soil moisture by minimizing the RMSE given in Eq. (15).

There are two possible sources of the errors in the estimated soil PSD. As described in the “Methods” section, the inverse method developed in this study is based on the relationship between spatial mean and standard deviation of soil moisture found in Pan and Peters-Lidard (2008). This relationship is valid as the spatial variations of vegetation and topography are less than that of soil, and the dominant factors controlling soil moisture spatial variations come from soils over the soil moisture sampling area. Although in this study the soil moisture data were collected in a small area (i.e., 80 m \times 160 m), vegetation and topography cannot be completely uniform, which implies that the spatial variation of vegetation and topography in the soil moisture sampling area can induce some errors in the estimated soil PSD. In addition to this error source, the uncertainty in the generalized soil-water potential relationship with soil-water content of Saxton et al. (1986) can also influence the accuracy of the estimated soil PSD because the relationship of Saxton et al. is used in this study to derive the standard deviation of soil moisture as a function of mean soil moisture state.

Summary

We developed and tested a simple method to retrieve soil PSD from observed soil moisture. This method is based on the relationship between spatial mean and standard deviation of soil moisture found in Pan and Peters-Lidard (2008). Using the generalized soil-water characteristics of Saxton et al. (1986), we de-

rived the standard deviation of soil moisture as a function of mean soil moisture state. In this function, we have seven parameters, i.e., mean and standard deviation of soil sand, clay, rock contents, and correlation coefficient between sand and clay. To estimate soil PSD we fitted the scatter plot of mean and standard deviation of soil moisture fields with the derived function.

We compared the estimated soil PSD with the measured PSD at one pit near our study domain. There is a good agreement between the inversely retrieved mean soil PSD and the measured soil PSD at the pit. We also found that the estimated mean and standard deviation of the rock contents are close to the measured values. In addition to these two comparisons, we conducted an error analysis to assess the parameter identifiability and reliability. The average values and 95% confidence limits of retrieved seven soil PSD parameters are close to the estimated true soil PSD values, which indicate that the proposed method is capable of inversely retrieving soil PSD from observed mean and standard deviation of soil moisture. Since there is no measurement of the standard deviation of soil sand and clay contents and correlation coefficient between sand and clay at WBW TDE sites, we could not perform a direct comparison between the estimated and measured values of those parameters. A future soil survey needs to be conducted over the WBW TDE sites.

As we apply the suggested method to retrieve soil PSD from observed soil moisture, two possible sources of error must be considered. The first concerns the contribution of spatial variation of vegetation and topography over the soil moisture sampling area to the soil moisture spatial distribution, which can produce error in the estimated soil PSD. The second possible source of error is the uncertainty in the generalized soil-water potential relationship with soil-water content of Saxton et al. (1986). Future research is needed to assess errors and uncertainties in the inversely estimated soil PSD due to spatial variation in vegetation and topography and the uncertainty in soil-water potential relationship with soil-water content.

Acknowledgments

The writers would like to thank P. J. Hanson for providing soil moisture and soil texture data used in this study, and four anonymous referees for their useful comments and suggestions. This research was partially supported by the Oak Ridge Associated Universities (ORAU) Ralph E. Powe Junior Faculty Enhancement Award (Pan).

Appendix

According to Saxton et al. (1986), soil moisture at saturation is given by

$$\theta_s = (1 - R/100)[c_1 + c_2S + c_3 \ln(C)/\ln(10)] \quad (16)$$

Take first- and second-order derivatives of θ_s with respect to sand (S), clay (C), and rock (R) contents as follows:

$$\frac{\partial \theta_s}{\partial S} = \left(1 - \frac{R}{100}\right)c_2; \quad \frac{\partial \theta_s}{\partial C} = \frac{(1 - R/100)c_3}{C \ln(10)}$$

$$\frac{\partial \theta_s}{\partial R} = -[c_1 + c_2S + c_3 \ln(C)/\ln(10)]/100 \quad (17)$$

$$\frac{\partial^2 \theta}{\partial S \partial C} = 0; \quad \frac{\partial^2 \theta_s}{\partial S^2} = 0; \quad \frac{\partial^2 \theta_s}{\partial C^2} = -\frac{(1-r/100)c_3}{C^2 \ln(10)}; \quad \frac{\partial^2 \theta_s}{\partial R^2} = 0 \quad (18)$$

Substituting Eqs. (17) and (18) into Eqs. (12) and (13), we have

$$\bar{\theta}_1 = (1 - \bar{R}/100)[c_1 + c_2 \bar{S} + c_3 \ln(\bar{C})/\ln(10)] - \sigma_C^2(1 - \bar{R}/100)c_3/[2\bar{C}^2 \ln(10)] \quad (19)$$

$$\sigma_1^2 = \sigma_S^2 \left(1 - \frac{\bar{R}}{100}\right)^2 c_2^2 + \sigma_C^2 \left(1 - \frac{\bar{R}}{100}\right)^2 c_3^2 / [\bar{C} \ln(10)]^2 + \sigma_R^2 \left[\frac{c_1 + c_2 \bar{S} + c_3 \ln(\bar{C})/\ln(10)}{100} \right]^2 + 2\rho_{S,C} \sigma_S \sigma_C c_3 (1 - \bar{R}/100)^2 / [\bar{C} \ln(10)] \quad (20)$$

As the pressure head ψ is between -10 and $-1,500$ kPa, Saxton et al. (1986) showed that the relationship between soil moisture and ψ is given by

$$\theta = (1 - R/100) \left(\frac{|\Psi|}{A} \right)^{1/B} \quad (21)$$

where $A = 100 \exp(c_4 + c_5 C + c_6 S^2 + c_7 S^2 C)$ and $B = c_8 + c_9 C^2 + c_{10} S^2 C$. Soil moistures at field capacity and wilting point correspond to $\psi = -33$ and $-1,500$ kPa, respectively. Same as saturated soil moisture, we take first- and second-order derivatives of soil moisture with regard to S , C , and R , which is shown in Eqs. (22)–(38), substitute those expressions into Eqs. (12) and (13), and finally obtain mean and standard deviation of soil moisture at field capacity or wilting point as a function of mean and standard deviation of sand, clay, and rock contents

$$\frac{\partial \theta}{\partial A} = \frac{1}{B} (1 - R/100) \left(\frac{\Psi}{A} \right)^{(1/B)-1} \left(-\frac{\Psi}{A^2} \right) = -\frac{\theta}{BA} \quad (22)$$

$$\frac{\partial \theta}{\partial B} = (1 - R/100) \left(\frac{\Psi}{A} \right)^{1/B} \left[\ln \left(\frac{\Psi}{A} \right) \right] \left(-\frac{1}{B^2} \right) = -\frac{\theta}{B^2} \ln \left(\frac{\Psi}{A} \right) \quad (23)$$

$$\frac{\partial \theta}{\partial R} = \left[-\left(\frac{\Psi}{A} \right)^{1/B} \right] / 100 \quad (24)$$

$$\frac{\partial^2 \theta}{\partial A^2} = \frac{(\partial \theta / \partial A)(BA) - \theta B}{(BA)^2} = \frac{\theta + B\theta}{B^2 A^2} \quad (25)$$

$$\frac{\partial^2 \theta}{\partial B^2} = -\ln \left(\frac{\Psi}{A} \right) \left[\frac{(\partial \theta / \partial B) B^2 - 2B\theta}{B^4} \right] = -\ln \left(\frac{\Psi}{A} \right) \left[\frac{-\theta \ln(\Psi/A) - 2B\theta}{B^4} \right] \quad (26)$$

$$\frac{\partial^2 \theta}{\partial R^2} = 0 \quad (27)$$

$$\frac{\partial A}{\partial S} = 100[\exp(c_4 + c_5 C + c_6 S^2 + c_7 S^2 C)](2c_6 S + 2c_7 S C) = A(2c_6 S + 2c_7 S C) \quad (28)$$

$$\frac{\partial A}{\partial C} = 100[\exp(c_4 + c_5 C + c_6 S^2 + c_7 S^2 C)](c_5 + c_7 S^2) = A(c_5 + c_7 S^2) \quad (29)$$

$$\frac{\partial B}{\partial S} = 2c_{10} S C; \quad \frac{\partial B}{\partial C} = 2c_9 C + c_{10} S^2 \quad (30)$$

$$\frac{\partial^2 A}{\partial S^2} = \frac{\partial}{\partial S} [A(2c_6 S + 2c_7 S C)] = A(2c_6 + 2c_7 C) + (2c_6 S + 2c_7 S C) \frac{\partial A}{\partial S} = A(2c_6 + 2c_7 C) + A(2c_6 S + 2c_7 S C)^2 \quad (31)$$

$$\frac{\partial^2 A}{\partial C^2} = \frac{\partial}{\partial C} [A(c_5 + c_7 S^2)] = (c_5 + c_7 S^2) \frac{\partial A}{\partial C} = A(c_5 + c_7 S^2)^2 \quad (32)$$

$$\frac{\partial^2 B}{\partial S^2} = \frac{\partial}{\partial S} (2c_{10} S C) = 2c_{10} C; \quad \frac{\partial^2 B}{\partial C^2} = \frac{\partial}{\partial C} (2c_9 C + c_{10} S^2) = 2c_9 \quad (33)$$

$$\frac{\partial \theta}{\partial S} = \frac{\partial \theta}{\partial A} \frac{\partial A}{\partial S} + \frac{\partial \theta}{\partial B} \frac{\partial B}{\partial S} = -\frac{\theta}{BA} A(2c_6 S + 2c_7 S C) - \frac{\theta}{B^2} \ln \left(\frac{\Psi}{A} \right) (2c_{10} S C) = -\frac{\theta}{B} (2c_6 S + 2c_7 S C) - \frac{2c_{10} S C \theta}{B^2} \ln \left(\frac{\Psi}{A} \right) \quad (34)$$

$$\frac{\partial \theta}{\partial C} = \frac{\partial \theta}{\partial A} \frac{\partial A}{\partial C} + \frac{\partial \theta}{\partial B} \frac{\partial B}{\partial C} = -\frac{\theta}{BA} A(2c_5 + c_7 S^2) - \frac{\theta}{B^2} \ln \left(\frac{\Psi}{A} \right) (2c_9 C + c_{10} S^2) = -\frac{\theta}{B} (2c_5 + c_7 S^2) - \frac{(2c_9 C + c_{10} S^2) \theta}{B^2} \ln \left(\frac{\Psi}{A} \right) \quad (35)$$

$$\frac{\partial^2 \theta}{\partial S \partial C} = \frac{\partial}{\partial S} \left(\frac{\partial \theta}{\partial C} \right) = \frac{\partial}{\partial S} \left[-\frac{\theta}{B} (2c_5 + c_7 S^2) - \frac{(2c_9 C + c_{10} S^2) \theta}{B^2} \ln \left(\frac{\Psi}{A} \right) \right] = \frac{(2c_6 S + 2c_7 S C)(2c_5 + c_7 S^2) \theta}{B^2} + \frac{2c_{10} S C (2c_5 + c_7 S^2) \theta}{B^3} \ln \left(\frac{\Psi}{A} \right) - \frac{2c_7 S \theta}{B} + \frac{2c_{10} S C (2c_5 + c_7 S^2) \theta}{B^2} + \frac{(2c_9 C + c_{10} S^2)(2c_6 S + 2c_7 S C) \theta}{B^3} \ln \left(\frac{\Psi}{A} \right) + \frac{2c_{10} S C (2c_9 C + c_{10} S^2) \theta}{B^4} \left[\ln \left(\frac{\Psi}{A} \right) \right]^2$$

$$\begin{aligned}
& + \frac{(2c_9C + c_{10}S^2)(2c_6S + 2c_7SC)\theta}{B^2} \\
& + \frac{4c_{10}SC(2c_9C + c_{10}S^2)\theta}{B^3} \ln\left(\frac{\Psi}{A}\right) - \frac{2c_{10}S\theta}{B^2} \ln\left(\frac{\Psi}{A}\right)
\end{aligned} \quad (36)$$

$$\begin{aligned}
\frac{\partial^2\theta}{\partial S^2} &= \frac{\partial}{\partial S} \left(\frac{\partial\theta}{\partial S} \right) = \frac{\partial}{\partial S} \left[-\frac{\theta}{B}(2c_6S + 2c_7SC) - \frac{2c_{10}SC\theta}{B^2} \ln\left(\frac{\Psi}{A}\right) \right] \\
&= \frac{(2c_6S + 2c_7SC)^2\theta}{B^2} + \frac{2(2c_6S + 2c_7SC)(2c_{10}SC)\theta}{B^3} \ln\left(\frac{\Psi}{A}\right) \\
&\quad - \frac{(2c_6 + 2c_7C)\theta}{B} - \frac{2c_{10}C\theta}{B^2} \ln\left(\frac{\Psi}{A}\right) + \frac{(2c_{10}SC)^2\theta}{B^4} \left[\ln\left(\frac{\Psi}{A}\right) \right]^2 \\
&\quad + \frac{2(2c_{10}SC)^2\theta}{B^3} \ln\left(\frac{\Psi}{A}\right) + \frac{2(2c_6S + 2c_7SC)(2c_{10}SC)\theta}{B^2}
\end{aligned} \quad (37)$$

$$\begin{aligned}
\frac{\partial^2\theta}{\partial C^2} &= \frac{\partial}{\partial C} \left(\frac{\partial\theta}{\partial C} \right) \\
&= \frac{\partial}{\partial C} \left[-\frac{\theta}{B}(2c_5 + c_7S^2) - \frac{(2c_9C + c_{10}S^2)\theta}{B^2} \ln\left(\frac{\Psi}{A}\right) \right] \\
&= \frac{(2c_5 + c_7S^2)^2\theta}{B^2} + \frac{(2c_5 + c_7S^2)(2c_9C + c_{10}S^2)\theta}{B^3} \ln\left(\frac{\Psi}{A}\right) \\
&\quad + \frac{(2c_5 + c_7S^2)(2c_9C + c_{10}S^2)\theta}{B^2} - \frac{(2c_9)\theta}{B^2} \ln\left(\frac{\Psi}{A}\right) \\
&\quad + \frac{(2c_9C + c_{10}S^2)(2c_5 + c_7S^2)\theta}{B^3} \\
&\quad + \frac{(2c_9C + c_{10}S^2)^2\theta}{B^4} \left[\ln\left(\frac{\Psi}{A}\right) \right]^2 + \frac{(2c_9C + c_{10}S^2)(c_5 + c_7S^2)\theta}{B^2} \\
&\quad + \frac{2(2c_9C + c_{10}S^2)(2c_{10}SC)\theta}{B^3} \ln\left(\frac{\Psi}{A}\right)
\end{aligned} \quad (38)$$

References

- Benjamin, J. R., and Cornell, C. A. (1970). *Probability, statistics, and decision for civil engineers*, McGraw-Hill, New York.
- Cambardella, C. A., et al. (1994). "Field-scale variability of soil properties in central Iowa soils." *Soil Sci. Soc. Am. J.*, 58, 1501–1511.
- Cary, P. W., and Chapman, C. H. (1988). "Automatic 1-D waveform inversion of marine seismic refraction data." *Geophys. J. R. Astron. Soc.*, 93, 527–5467.
- Chang, D. H., and Islam, S. (2000). "Estimation of soil physical properties using remote sensing and artificial neural network." *Remote Sens. Environ.*, 74, 534–544.
- Chang, D.-H., Kothari, R., and Islam, S. (2003). "Classification of soil texture using remote sensed brightness temperature over the Southern Great Plains." *IEEE Trans. Geosci. Remote Sens.*, 41, 664–674.
- Edmonds, W. J., Campbell, J. B., and Lentner, M. (1985). "Taxonomic variation within three soil mapping units in Virginia." *Soil Sci. Soc. Am. J.*, 49, 957–961.
- Edmonds, W. J., Iyengar, S. S., Zelazny, L. W., Lentner, M., and Peacock, C. D. (1982). "Variability in family differentia of soils in a second order soil survey mapping unit." *Soil Sci. Soc. Am. J.*, 46, 88–93.

- Edmonds, W. J., and Lentner, M. (1986). "Statistical evaluation of the taxonomic composition of three soil map units in Virginia." *Soil Sci. Soc. Am. J.*, 50, 997–1001.
- Feddes, R. A. (1995). "Remote sensing—Inverse modeling approach to determine large scale effective soil hydraulic properties in soil-vegetation-atmosphere systems." *Space and time scale variability and interdependencies in hydrological processes: International hydrology series*, Cambridge Univ. Press, Cambridge, U.K., 33–42.
- Fletcher, R. (1987). *Practical methods of optimization*, Wiley Interscience, Chichester, NY.
- Hanson, P. J., Todd, D. E., Edwards, N. T., and Huston, M. A. (2003). "Walker Branch Throughfall Displacement Experiment." *North American temperate deciduous forest responses to changing precipitation regimes: Ecological studies*, P. J. Hanson and S. D. Wullschlegel, eds., Vol. 166, Springer, New York, 8–31.
- Hanson, P. J., Todd, D. E., Huston, M. A., Joslin, J. D., Croker, J., and Rugé, R. M. (1998). "Description and field performance of the Walker Branch Throughfall Displacement Experiment: 1993–1996." *ORNL TM-13586*, Oak Ridge National Laboratory, Oak Ridge, TN.
- Keilis-Borok, V. J., and Yanovskaya, T. B. (1967). "Inverse problems in seismology (structural review)." *Geophys. J. R. Astron. Soc.*, 13, 223–234.
- Kim, C. P., Stricker, J. N. M., and Feddes, R. A. (1997). "Impact of soil heterogeneity on the water budget of the unsaturated zone." *Water Resour. Res.*, 33(5), 991–999.
- Koren, Z., Mosegaard, K., Landa, E., Thore, P., and Tarantola, A. (1991). "Monte Carlo estimation and resolution analysis of seismic background velocities." *J. Geophys. Res.*, 96, 20289–20299.
- Landa, E., Beydoun, W., and Tarantola, A. (1989). "Reference velocity model estimation from prestack waveforms: Coherency optimization by simulated annealing." *Geophysics*, 54, 984–8990.
- Milly, P. C. D., and Eagleson, P. S. (1987). "Effects of spatial variability on annual average water balance." *Water Resour. Res.*, 23(11), 2135–2143.
- Mosegaard, K., and Tarantola, A. (1995). "Monte Carlo sampling of solutions to inverse problems." *J. Geophys. Res.*, 100, 12431–12447.
- Mosegaard, K., and Vestergaard, P. D. (1991). "A simulated annealing approach to seismic model optimization with sparse prior information." *Geophys. Prospect.*, 39, 599–611.
- Palacios-Orueta, A., and Ustin, S. L. (1998). "Remote sensing of soil properties in the Santa Monica Mountains. 1: Spectral analysis." *Remote Sens. Environ.*, 65, 170–183.
- Pan, F., and Peters-Lidard, C. D. (2008). "On the relationship between mean and variance of soil moisture fields." *J. Am. Water Resour. Assoc.*, 44(1), 235–242.
- Peters, L. N., Grigal, D. F., Curlin, J. W., and Selvidge, W. J. (1970). "Walker Branch Watershed Project: Chemical, physical and morphological properties of the soils of Walker Branch Watershed." *ORNL-TM-2968*, Oak Ridge National Laboratory, Oak Ridge, Tenn.
- Press, F. (1968). "Earth models obtained by Monte Carlo inversion." *J. Geophys. Res.*, 73, 5223–5234.
- Rawls, W. J., Brakensiek, D. L., and Savabi, R. (1989). "Infiltration parameters for rangeland soils." *J. Range Manage.*, 42(2), 139–142.
- Rawls, W. J., Brakensiek, D. L., and Saxton, K. E. (1982). "Estimation of soil water properties." *Trans. Am. Soc. Agric. Engrs*, 25, 1316–1330.
- Rothman, D. H. (1986). "Automatic estimation of large residual statics corrections." *Geophysics*, 51, 332–346.
- Rothman, R. H. (1985). "Nonlinear inversion, statistical mechanism, and residual statistics estimation." *Geophysics*, 50, 2784–2807.
- Santamarina, J. C., and Fratta, D. (1998). *Introduction to discrete signals and inverse problems in civil engineering*, ASCE, Reston, Va.
- Saxton, K. E., Rawls, W. J., Romberger, J. S., and Papendick, R. I. (1986). "Estimating generalized soil water characteristics from texture." *Trans. Am. Soc. Agric. Engrs*, 50, 1031–1035.
- Sharma, M. L., and Luxmoore, R. J. (1979). "Soil spatial variability and

- its consequences on simulated water balance." *Water Resour. Res.*, 15(6), 1567–1573.
- USDA-SCS. (1982). "Procedures for collecting soil samples and methods of analysis for soil survey." *Soil Survey Investigations Report 1*, Washington, D.C.
- Yeh, T.-C. J. (1989). "One-dimensional steady state infiltration in heterogeneous soils." *Water Resour. Res.*, 25(10), 2149–2158.
- Young, F. J., Hammer, R. D., and Williams, F. (1997). "Estimating of map unit composition from transect data." *Soil Sci. Soc. Am. J.*, 61, 854–861.
- Young, F. J., Hammer, R. D., and Williams, F. (1998). "Evaluating central tendency and variance of soil properties within map units." *Soil Sci. Soc. Am. J.*, 62, 1640–1646.
- Zhu, J., and Mohanty, B. P. (2003). "Effective hydraulic parameters for steady state vertical flow in heterogeneous soils." *Water Resour. Res.*, 39, 1227.